HHS Public Access

Author manuscript

Cancer Res. Author manuscript; available in PMC 2017 July 01.

Published in final edited form as:

Cancer Res. 2016 July 1; 76(13): 3851–3861. doi:10.1158/0008-5472.CAN-15-3358.

Constitutive activation of PI3K in oocyte induces ovarian granulosa cell tumors

So-Youn Kim[1,4], **Katherine Ebbert**[1], **Marilia H. Cordeiro**[1], **Megan M. Romero**[1], **Kelly A. Whelan**[1], **Adrian A. Suarez**[2], **Teresa K. Woodruff**[1], and **Takeshi Kurita**[3,4]

[1]Division of Reproductive Science in Medicine, Department of Obstetrics and Gynecology, Feinberg School of Medicine, Northwestern University, Chicago IL

[2]Department of Pathology, The Comprehensive Cancer Center, Ohio State University, Columbus OH

[3]Department of Molecular Virology, Immunology & Medical Genetics, The Comprehensive Cancer Center, Ohio State University, Columbus OH

Abstract

Cell-cell interactions play crucial roles in the maintenance of tissue homeostasis, a loss of which often leads to varying diseases, including cancer. Here, we report that uncontrolled PI3K activity within oocytes irreversibly transforms granulosa cells (GC), causing GC tumors (GCT) through perturbed local cell-communication. Previously, we reported reproductive phenotypes of transgenic mice, in which expression of constitutively active mutant PI3K was induced in primordial oocytes by Gdf9-iCre. The transgenic mice (Cre+) demonstrated severe ovarian phenotypes, including the overgrowth of excess ovarian follicles and anovulation. Surprisingly, the Cre+ mice became cachectic by postnatal day 80 due to bilateral GCT. Although GCT cells proliferated independently of oocytes, local interactions with mutant PI3K-positive oocytes during early folliculogenesis were essential for the GC transformation. Growing GCT cells expressed high levels of inhibin βA and nuclear SMAD3, and the proliferation rate was positively correlated with a high activin A to inhibin A ratio. These results suggested that the tumor cells stimulated their growth through an activin A autocrine signaling pathway, a hypothesis confirmed by activin A secretion in cultured GCT cells which proliferated in response. Although communication between the oocyte and surrounding somatic cells is critical for the normal development of ovarian follicles, perturbations in oocyte-GC communication during early folliculogenesis can induce GCT by activating an autocrine growth circuit program in GC.

Keywords

cell-cell interaction; mouse model; granulosa cell tumor; PI3K; Activin A

[4]CORRESPONDING AUTHORS: So-Youn Kim, Ph.D., Northwestern University Feinberg School of Medicine, Department of Obstetrics and Gynecology, Lurie Building 10-250, 303 East Superior Street, Chicago, IL 60611, Phone: 312-503-2530, so-youn-kim@northwestern.edu. Takeshi Kurita, Ph.D., Department of Molecular Virology, Immunology & Medical Genetics, The Comprehensive Cancer Center, Ohio State University, Biomedical Research Tower Room 812, 460 West 12th Avenue, Columbus, OH 43210, Phone: 614-685-8502, takeshi.kurita@osumc.edu.

DISCLOSURE

The authors disclose no potential conflicts of interest.

INTRODUCTION

Granulosa cell tumors (GCTs) are sex cord stromal-tumors that constitute approximately 5% of human ovarian tumors (1,2). For the high recurrence and mortality rates (3,4), the development of effective treatments or early detection markers for GCTs is of utmost importance. The two types of GCTs display different pathologies: adult GCTs (AGCTs) are common in peri/post-menopausal women, whereas juvenile GCTs (JGCTs) develop in juvenile girls and young women (5,6). The C402G missense mutation in *FOXL2* is found in over 90% of AGCTs, although the same mutation is detected in less than 10% of JGCTs (7–9), indicating their distinctive etiologies. Recent studies detected recurrent in-frame duplications in exon 3 of *AKT1* gene in JGCTs (10,11). In mice, loss of negative regulators of the PI3K-AKT pathway, PTEN and FOXO1/3 in GCs, resulted in GCTs (12), suggesting the crucial role of the PI3K-AKT pathway in the pathogenesis of JGCTs.

In normal folliculogenesis, the levels of oocytic phosphatidylinositol 3,4,5-trisphosphate (PIP3) determine the activation and survival of primordial follicles (13). When elevated PIP3 activates a primordial oocyte, the pregranulosa cells associated with the active oocyte differentiate into GCs, forming primary follicles. In activated follicles, the growth and differentiation of GCs are under the control of autocrine, paracrine and endocrine factors (14), and multiple TGFβ family ligands and inhibitors play critical roles in all three modes of regulatory mechanism (15,16). Among TGFβ superfamily members, inhibins and activins are particularly important in the maintenance of reproductive functionality by mediating signaling in the hypothalamus-pituitary-gonad (HPG) axis (17–20). Heterodimmers of inhibin α and βA or βB subunits form Inhibin A or B, respectively, and homodimers or heterodimer of βA and βB can form activin A and B or AB, respectively. In female mammals, the α, βA and βB subunits are primarily produced in GCs and pituitary. Activins positively regulate FSH (follicle-stimulating hormone) synthesis and secretion in pituitary, and inhibins act as a negative regulator by competing with activins for their type II receptors. Since FSH regulates growth and differentiation of GCs, loss of inhibin αover-stimulates the follicles through overproduction of FSH, resulting in sex cord-stromal tumors of GC origin (21). The growth of sex cord tumors in *Inha* null mice were attenuated by overproduction of follistatin, a natural antagonist of activins, indicating that the phenotypes of *Inha* null mice were due to unantagonized activin-actions (22). Furthermore, overexpression of inhibin α chain in hepatocytes caused the arrest of ovarian follicles at the early antral stage through suppression of pituitary FSH (23), demonstrating the significance of the balance between inhibin and activin in ovarian physiology.

The canonical TGFβ family signaling is transduced by SMAD transcription factors, and the phenotypes of SMAD mutant mice highlight the importance of TGFβ family pathways in the physiology of GCs: Deletion of *Smad1* and *Smad5* in GCs induced GCTs (24,25), however the tumor formation was inhibited by a concomitant loss of *Smad3* (26). Thus, BMP-regulated SMADs (SMAD1/5/9) and TGFβ/activin-regulated SMADs (SMAD2/3) have antagonistic functions in GCs. Unfortunately, the exact function of specific TGFβ superfamily members and their signaling in GCT pathogenesis is not fully elucidated. Here

we report the development of GCTs through the activation of activin A (ActA)-mediated autocrine-growth circuit in GCs as a consequence of PI3K activation in primordial oocytes.

MATERIALS AND METHODS

Animals

All procedures involving mice were approved by the IACUC at Northwestern and Ohio State University. Oocyte-specific transgenic mice for constitutively active PI3K (PIK3CA*) were generated as previously described (27). Homozygous female mice for Cre-inducible knock-in allele for *Pik3ca** (28) were crossed with heterozygous *Gdf9-iCre* or *Zp3-Cre* (29) male mice (Jackson Laboratories, Bar Harbor, ME). The expression of PIK3CA* and enhanced green fluorescent protein (EGFP) was induced as Cre removed the Loxp-stop-Loxp cassette upstream of *Pik3ca*-ires-EGFP.* The positive and negative for *Gdf9-iCre* were referred to as Cre+ and Cre−, respectively, and the Cre-were used as littermate controls. Because Cre+ mice were euthanized as soon as they demonstrated cachexia, there was a two week-range (PD70-85) in age for the tissue collection after PD65. The effect of PIK3CA* expression in activated oocytes was addressed utilizing *Zp3-Cre* mice.

Pathological analysis

Histology and cellular morphologies of tumors were evaluated in H&E stained sections by an experienced gynecologic pathologist (AAS).

Immunostaining and Immunoblot analysis

Immunofluorescence (IF), immunohistochemistry (IHC) and immunoblot analysis were performed as previously described (27). The concentration and the manufacturers of primary antibodies are listed in Supplementary information.

Subrenal grafting

Subrenal grafting of mouse ovaries was performed as previously described (27,30). Ovaries from PD5 Cre− and Cre+ mice were grafted onto contralateral kidneys of ovariectomized (OVX) NOD.Cg-*Prkdc*^{scid} *Il2rg*^{tm1Wjl}/SzJ mice (The Jackson Laboratory) as one ovary per kidney in three combinations; left kidney/ right kidney = Cre−/Cre−, Cre−/Cre+, and no(Sham operated with no graft)/Cre+. Transplants were collected 70 days after grafting.

For GCT grafts, adult female nude mouse hosts (The Jackson Laboratory) were used. Tumors from Cre+ mice were cut into ~1mm^3 in iced DMEM (Life Technologies, Carlsbad, CA), and grafted into OVX or sham-operated (Sham) hosts (4 pieces/mice). Transplants were collected 35 days later. Experiments were repeated with tumor tissues from ≥3 different Cre+ donor mice and ≥7 hosts/group. Tumor take rate was calculated for each host by number of grown-tumor/4 grafts.

Isolation of oocytes from PD35 mouse ovaries

Oocytes were isolated by puncturing the PD35 ovaries with 27-gauge needles in L15 media (Life Technologies). Isolated oocytes were washed with PBS containing 3mg/ml

Polyvinylpyrrolidone (Sigma-Aldrich, St. Louis, MO), and stored at −80°C for genomic DNA (gDNA) isolation.

PCR genotyping

Primer sequences to detect active (Stop-Deleted) and inactive (Stop-Floxed) transgenic alleles are as follows: F, CACAGCTCGCGGTTGAGG; R1, TGCTCGACGTTGTCACTGAA; R2, CGGGTGTACTCCTCATATAACA. *Gapdh* was used for quality control of gDNA. gDNA was isolated from GCT grafts, as well as control tissues including oocytes from PD35 Cre+ ovary, tails from PD5 Cre− and Cre+ mice, and PD65 Cre+ ovaries. PCR was performed with 10ng gDNA. The thermal cycler was programmed as follows: 94°C, 5min; [94°C, 15sec: 56°C, 1min: 72°C, 1min] ×40 cycles; 72°C, 7min.

Serum hormone measurement

Blood was collected by cardiac puncture. The activin and inhibin levels were determined by the Sandwich enzyme-linked immunosorbent assay using ActA, inhibin A (InhA) and inhibin B ELISA kits (Anshlab, Webster, TX). LH, FSH, anti-Müllerian hormone (AMH), 17β-estradiol and testosterone were measured at the University of Virginia Ligand Core Facility. The hormone measurements were repeated with sera from at least 4 different mice/group.

Primary culture of granulosa and GCT cells

Ovaries from Cre− and GCT pieces from Cre+ mice (PD70) were digested into single cells by shaking in Hank's Balanced Salt Solution (HBSS) (Life Technologies) containing 10mg/ml collagenase (Worthington Biochemical Corporation, Lakewood, NJ), 1mg/ml bovine testes hyaluronidase (Type IV-S, Sigma-Aldrich), and 200mg/ml DNase I (Worthington Biochemical). Collected cells were incubated with RBC Lysing Buffer Hybri-Max™ (Sigma-Aldrich) and then seeded on 60mm culture dish, coverslips (22× 22mm, VWR, Radnor, PA) or 96-well plates coated with poly-L-lysine (Sigma-Aldrich) in DMEM/F-12 medium (Life Technologies, supplemented with Insulin-transferrin-sodium selenite, I1884, Sigma-Aldrich) containing 10% heat-inactivated FBS (Mediatech Inc., Manassas, VA). After 24 hours, cells were incubated in DMEM/F-12 medium with 1% FBS for 48 hours before subjected to the assays. Since GCT cells did not grow in FBS containing medium, experiments were repeated with freshly isolated GC and GCT cells from >5 different donors.

For immunocytochemistry, 1×10^4 cells on coverslips were treated with 1% FBS, 25ng/ml recombinant human ActA (31) and/or 3μg/ml recombinant human follistatin 288 (FST) (Dr. Albert Parlow) for 48 hours. Cells fixed with methanol were washed and permeabilized with 1% Tween20-PBS.

For hormone measurements, conditioned-media were collected from 96-well plates with 0.5×10^4 cells/well at 24 hours after medium change.

For proliferation assay, 1×10^4 cells/well were incubated with serum-free DMEM/F-12 medium containing PBS (control) or 25ng/ml ActA in 96-well plates for 48 hours, and the cell-density was measured by CellTiter 96® Assay kit (Promega, Madison, WI).

Statistical analysis

All statistical analyses were performed using Prism 4.0 software (GraphPad Software, San Diego, CA). Two-tailed and unpaired t-tests were used for analyses of serum hormone levels. Ovarian weight, hormone levels in the host mice and proliferation assay were analyzed with one-way ANOVA in conjunction with Post-hoc analysis with Tukey's Multiple Comparison Test. Statistical significance was marked with *, $P<0.05$: **, $P<0.01$ and ***, $P<0.001$. $P>0.1$ was marked as ns (non-significant).

RESULT

Oocytic PI3K activity transforms GCs

When Cre+ mice were examined at PD65, bilateral ovarian tumors were present with 100% penetrance (n≥35) (Fig. 1A). The tumors appeared as solid masses with hemorrhagic cysts, typical for ovarian sex cord-stromal tumors (Fig. 1B). Tumors weighed 200× heavier than PD65 Cre− ovaries (Fig. 1C). At PD50, tumors were undetectable in Cre+ ovaries (n=10) (Fig. 1Da) (27), indicating the highly proliferative nature of the tumor (Fig. 1Db). The tumor development was followed up to PD85, by when all Cre+ mice were euthanized due to cachectic weight-loss.

In the Cre+ ovaries, non-tumor tissues such as hemorrhagic cysts (Fig. 1Ea) and secondary follicles (Fig. 1Eb) were rare as the entire ovary was permeated with tumor cells (Fig. 1Ec). Some tumor cells were still contained within the mural GC (mGC) lining (Fig. 1Ed), suggesting their GC origin. While the cord-like architecture (Fig. 1Ee) exhibited striking similarity to human AGCTs, other characteristics resembled to JGCTs, which typically lack abundant nuclear grooves and Call-Exner bodies. The presence of follicle-like cysts was also similar to human JGCTs (Fig. 1Ef) (32). Based on the cellular morphology and the absence of FOXL2 mutation, our model appeared to reflect the biology of JGCTs. The ambiguous histopathological classification of the mouse tumor reflects the natural history of these GCTs, which arise from multiple follicles whereas human GCTs likely develop through clonal expansion of mutant cells.

Expression of FOXL2 and inhibin α further confirmed that the cord-like cell masses were GCTs (Fig. 2A). The tumor cells uniformly expressed KI67 and SMAD3 (Fig. 2A, Cre+), which are normally restricted to GCs in the growing follicles (Fig. 2A, Cre−). Immunoblotting analysis detected overexpression of inhibin βA (33), SMAD3 (34), and GATA4 (35) in Cre+ ovaries, which are often up-regulated in human GCTs (Fig. 2B).

The transformed GCs in PD65 Cre+ ovaries maintained high levels of p-AKT even though they were not associated with oocytes (Fig. 2C, Cre+). To test if high p-AKT levels in GCTs reflected the altered endocrine profile of Cre+ mice, serum hormone levels were examined. AMH, a marker for GCTs (36), was significantly higher in Cre+ mice (Fig. 2D). As suggested by the nuclear SMAD3 and cachexia, ActA was also elevated (Fig. 2D). However,

in Cre+ mice FSH was significantly lowered, whereas testosterone, 17β-estradiol and InhA were significantly elevated despite the lowered FSH (Fig. 2D). These observations suggest that Cre+ oocytes alter the GCs to maintain high growth and hormone-secreting activities independently of oocytic and endocrine factors.

GCT growth was independent of oocytic factors

The oocyte-independent growth of GCTs was further assessed by grafting pieces of GCTs devoid of healthy oocytes, onto the kidneys of immunodeficient OVX mice. This also evaluates if the altered endocrine environment of Cre+ mice is required for the growth of GCTs. The GCT pieces developed into large tumors (Fig. 3A), maintaining aforementioned histology (Fig. 3B). The tumor cells invaded into host kidneys (Fig. 3Ci), and renal tubules and glomeruli were found within GCTs (Fig. 3Cii & iii). The GCT markers were also maintained (Fig. 3D). Among inhibin chains, the βA was the predominant subunit and uniformly expressed throughout the tumor, whereas α and βB subunits were detected only in a subset of cells (Fig. 3D). Thus, the serum concentration of ActA was significantly elevated in the tumor hosts compared to normal mice (supplementary Fig. S1). Interestingly, a substantial portion of tumor cells expressed FOXO1, PTEN and p-SMAD1/5/9 (Fig. 3D). Thus, the loss of these negative growth regulators was not involved in the pathogenesis of GCTs in this mouse model.

GCTs do not express mutant PI3K transgene

As assessed by EGFP reporter, *Gdf9-iCre* activated *Pik3ca*-ires-EGFP* transgene in oocytes (27) (supplementary Fig. S2) and a subpopulation of ovarian surface epithelial cells (OSECs), which were marked with KRT8 (Fig. 3Ei). In Cre+ ovaries, PIK3CA*-positive OSECs appeared hypertrophic, but remained on the ovarian surface, demonstrating no sign of tumorigenesis and stromal invasion (Fig. 3Ei and ii). KI67 staining was also absent (Fig. 3Eiii). Some GCT transplants contained EGFP-positive OSECs in peripheral regions (Fig. 3Eiii). However, OSECs remained predominantly negative for KI67 (Fig. 3Eiv), suggesting that the constitutive activation of PI3K is insufficient for malignant transformation of OSECs.

The absence of *Pik3ca** transgene activation in GCTs was further confirmed by PCR (Fig. 3Fi and ii). The PCR assay by 30 cycles, which was sufficient to detect the active alleles in the positive controls (Cre+ oocytes and ovaries), failed to detect the active allele in all GCT transplants (not shown). By 40 cycles, a faint band (Fig. 3Fiii, red asterisk) for the active transgene was detected in GCT transplants that contained EGFP-positive OSECs (Fig. 3Fiii, GCT#2), while other GCT transplants were negative (Fig. 3Fiii, GCT#1). Meanwhile, all GCT transplants were clearly positive for the inactive allele (Fig. 3Fiii, blue asterisks) suggesting that the faint active-allele band was likely from contaminated OSECs. Hence, the development of GCT was independent of PIK3CA* expression in GCs.

Intra-ovarian interaction with mutant oocytes is essential for the transformation of GCs

In mice, GCTs can be initiated solely by perturbation of HPG axis, particularly the unopposed action of gonadotropins (37). Since the endocrine profile of Cre+ mice was significantly altered by PD35 (27), we tested the possibility that the altered endocrine milieu

triggers ovarian tumorigenesis in Cre+ mice. Immature PD5 ovaries were grafted into the contralateral kidneys of OVX nude mice in the following combinations (one ovary/kidney); right kidney/left kidney = Cre−/Cre−, Cre−/Cre+ and no (no graft)/Cre+. In this assay, immature ovaries grafted on left and right kidneys are exposed to the identical endocrine milieu throughout development, thus the contribution of genetic and endocrine factors to tumorigenesis can be assessed. In Cre−/Cre+ group, co-grafting did not affect the prevalence of GCTs in Cre− and Cre+ ovaries: none of Cre− ovaries (n=5) showed overgrowth or signs of tumorigenesis (Fig. 4A), whereas all five Cre+ ovaries developed GCTs (Fig. 4B). Thus, the endocrine environment that is permissive for GCT formation in Cre+ ovary is insufficient to initiate GCTs in Cre− ovaries. It emphasized the critical role of local interactions with mutant oocytes for the transformation of GCs.

On the other hand, co-grafting of Cre+ ovary inhibited the development of large antral follicles and corpus lutea in Cre− ovaries (Fig. 4A), suggesting the repression of the HPG-axis by Cre+ ovaries through the over-production of hormones. Likewise, the Cre− ovary endocrinely attenuated the growth of GCTs in Cre+ ovaries (Fig. 4B). Thus, the KI67 labeling index of GCTs (Fig. 4C and D), and serum AMH level were higher in no/Cre+ than Cre−/Cre+ group (Fig. 4E). To identify the endocrine factors affecting GCT growth, the hormone profiles of host mice were compared (Fig. 4E). LH was below detection limit in all samples except two out of five Cre−/Cre− group (not shown). Thus, it was excluded from the analyses. FSH, estradiol and testosterone were equally reduced in Cre−/Cre+ and no/Cre+ groups compared to Cre−/Cre− group. In contrast, the serum ActA level was significantly increased in Cre−/Cre+ and no/Cre+ groups. Because inhibin antagonizes activin actions, the ratio between ActA and InhA should more accurately indicate the overall activin activity than serum concentration of each hormone. Although it was not statistically significant, the ratio of ActA over InhA was higher in no/Cre+ than Cre−/Cre+ group (Fig. 4F). Most importantly, the ratio of ActA/InhA showed strong positive correlation with KI67 labeling index (r^2= 0.784, F-test= 62.01) (Fig. 4G). The p-SMAD3 positivity in GCTs was also higher in no/Cre+ than Cre−/Cre+ group (Fig. 4C), suggesting that ActA-SMAD3 pathway stimulates the growth of GCTs.

GCT is initiated in primordial and primary follicles

The co-grafting experiment indicated the essential role of intra-ovarian interaction with Cre+ oocytes in GCT development. However, the activation of oocytic PI3K by Zp3-Cre in secondary follicles showed no detectable abnormalities in ovaries such as follicle overgrowth, hemorrhagic cysts or GCTs by PD90 (n=24, Fig. 5A and B). Therefore, the interaction with PI3K-mutant oocytes at primordial/primary follicle stages appears essential for the transformation of GCs.

Accordingly, we examined neonatal and prepubertal Cre+ and Cre− mouse ovaries for changes in the expression patterns of inhibin α and βA as well as markers for PI3K-AKT activity. Both inhibin βA and inhibin α were slightly elevated in the pregranulosa cells of PD5 Cre+ ovaries, indicating that the PI3K activation in oocytes affects the physiology of GCs within primordial follicles (Fig. 5C). In contrast, p-AKT expression in primordial follicles was comparable between Cre+ and Cre− ovaries. However, p-AKT was elevated in

oocytes and GCs of Cre+ ovaries after primary follicle transition (Fig. 5D) (27). The GCs in Cre+ ovaries maintained the expression of PTEN and FOXO1 throughout folliculogenesis (supplementary Fig. S3), confirming that loss of these tumor suppressors is not the cause of GCT formation.

Effect of HPG-axis activity on GCT growth

The GCT-grafts grew into large tumors in OVX hosts (Fig. 3), where the elevated FSH likely stimulated the initial growth of tumor pieces (38). To address whether the endocrine environment of the OVX host is essential for growth, the GCT pieces were transplanted into Sham-operated nude mice, where the gonadotropin levels are tightly controlled by the HPG axis. The overall tumor take rate was reduced in the Sham compared to OVX group (Fig. 6A and B), suggesting that high FSH in the OVX hosts facilitated the initial survival of tumor explants, presumably by promoting angiogenesis (39). Similarly to the co-grafting experiment, growth of GCT-grafts was attenuated by the presence of intact ovaries (Fig. 6A and supplementary Figs. S4 and S5). This reflected the significantly lower ratio of ActA over InhA in Sham hosts (Fig. 6C), in which the HPG axis appeared to counteract excess ActA by stimulating normal ovaries to produce InhA.

ActA stimulates growth of GCT cells *in vitro*

To assess if GCT cells autocrinely stimulate their growth by production of ActA, GCT cells were cultured *in vitro*. Both cultured GCs and GCT cells secreted detectable levels of ActA and InhA (Fig. 7A and B). However, GCT cells secreted 40× more of ActA than normal GCs, while InhA showed no significant difference. Although ActA was secreted into the medium, the primary GCT cells were growth-quiescent (Fig. 7C and D), and supplementation of recombinant ActA at 25ng/ml was required to stimulate growth (Fig. 7D). The absence of autocrine growth-stimulation was likely due to the fast diffusion of ActA in the 2D culture condition. The specificity of recombinant ActA was confirmed by inhibition of KI67 expression by FST (Fig. 7C). Interestingly, recombinant ActA stimulated the production of inhibin α, suggesting that the transformed GCs maintained cell-autonomous feedback mechanisms to attenuate activin-action. While ActA induced nuclear accumulation of p-SAMD3, it had no effect on p-AKT. FBS did not stimulate growth or pSMAD3 in GCT cells, suggesting that the growth of GCTs in our mouse model is highly dependent on ActA-SMAD3 pathway (Fig. 7E).

DISCUSSION

Ovarian follicles undergo an organogenesis called folliculogenesis, which involves growth, differentiation and apoptosis of somatic cells. Our current study demonstrates for the first time that perturbed communication with oocytes during folliculogenesis can irreversibly transform GCs leading to GCTs.

It is widely accepted that perturbation in organogenesis can result in precancerous conditions. The development of vaginal adenocarcinoma by in utero exposure to diethylstilbestrol is the best-documented clinical cases of such transformation: diethylstilbestrol causes precancerous lesions by altering epithelial cell fate through

disruption of cell-cell communication (40). Ovarian malignancies developed in *Fancd2* and *Dazl* null mutant mice from altered micro and endocrine environments through premature oocyte loss (41). These studies affirm the pivotal role of oocytes in the maintenance of ovarian homeostasis and the repression of malignancies. Our current study provides another example of the malignant transformation of non-mutant cells by abnormal cell-communication. Thus, there is a concern that exogenous factors, such as chemical exposure, may initiate GCTs by disrupting cell-communications during folliculogenesis.

How oocytic PI3K activity transforms GCs remains unclear. Since ActA action on normal GCs depends on FSH (42–44), loss of gonadotropin dependency is likely a critical step in GC tumorigenesis. Oocytic PI3K activation elevated p-AKT in Cre+ oocytes as well as associated GCs from primary to antral stages. However, large hydrophobic molecules such as PIP3 cannot pass through gap junctions and intercellular exchange of plasma membrane components through lateral diffusion is not documented. Hence, we hypothesize that the communication between Cre+ oocytes and GCs is mediated by paracrine molecules that activate AKT in GCs: PI3K activity promotes oocyte to secrete paracrine factors, and the continuous exposure to the oocytic factors irreversibly alters physiology of GCs to secrete and respond to ActA independently of FSH. As GCs transform, AKT activity is also maintained independently of gonadotropins and oocytic factors. Meanwhile, we do not exclude the possibility that PIP3 is directly transferred to GCs through an unknown mechanism as a recent study suggests that RNAs can be transferred from GC to oocytes through transzonal projections (45).

The elevation of AKT activity itself may play a role in the establishment of an ActA autocrine growth-circuits, and thus mutations that activate PI3K-AKT pathway in GCs may initiate GCTs. In this regard, reported *AKT1* mutations in JGCTs (11) may contribute to the establishment of ActA autocrine circuit in GCs. On the other hand, the role of *GNAS* R201 mutations, which constitutively activate G protein-coupled receptors (46), can be explained by constitutive FSH receptor signaling that sensitizes GCs to ActA-induced proliferation in JGCTs (9).

Development of GCTs has been observed in genetic mouse models: null mice for *Inhα* (21), *Esr2* (47), mice with GC-specific activating mutation in *Ctnnb1* (48), and GC-specific null mutation in *Smad1/Smad5* (25), *Foxo1/Foxo3 and Foxo1/Foxo3/Pten* (12). Although these mutations have not been detected in human GCTs, these mice are excellent tools to understand the signaling pathways that are potentially involved in the pathogenesis of human GCTs. Unfortunately, the efficacy of these models in drug testing is limited as GCTs are insensitive to certain signaling pathways due to the causal mutations. Although it is unclear from current studies if elevated oocytic PIP3 causes human GCTs, our mouse GCT model may well be suited to address this gap in therapeutic testing as the tumor cells do not carry genetic mutations. A recent clinical study identified the association between circulating ActA and the presence of the anorexia/cachexia syndrome in cancer patients (49). However, other factors, such as cytokines, are well documented in cancer cachexia (50). Our mouse model expressing high ActA is useful to determine the role of ActA in GCTs as well as cachexia. The usefulness of this mouse strain for preclinical studies, however, will be established by further comparative studies to human GCTs.

Supplementary Material

Refer to Web version on PubMed Central for supplementary material.

Acknowledgments

FINANCIAL SUPPORT

This work was supported by the Center for Reproductive Health After Disease (P50HD076188) from the National Institutes of Health National Center for Translational Research in Reproduction and Infertility (NCTRI) (S.Y. Kim, K. Ebbert, M.H. Cordeiro, M.M. Romero, K.A. Whelan, T.K. Woodruff and T. Kurita), and Granulosa Cell Tumour Research Foundation (S.Y. Kim), R01CA154358 and P30CA016058 Cancer Center Support grant (T. Kurita) and P50HD28934 (UVA Center for Research in Reproduction Ligand Assay and Analysis Core).

References

1. Schumer ST, Cannistra SA. Granulosa cell tumor of the ovary. J Clin Oncol. 2003; 21:1180–9. [PubMed: 12637488]
2. Pectasides D, Pectasides E, Psyrri A. Granulosa cell tumor of the ovary. Cancer Treat Rev. 2008; 34:1–12. [PubMed: 17945423]
3. Sehouli J, Drescher FS, Mustea A, Elling D, Friedmann W, Kuhn W, et al. Granulosa cell tumor of the ovary: 10 years follow-up data of 65 patients. Anticancer Res. 2004; 24:1223–9. [PubMed: 15154651]
4. Colombo N, Parma G, Zanagnolo V, Insinga A. Management of ovarian stromal cell tumors. J Clin Oncol. 2007; 25:2944–51. [PubMed: 17617526]
5. Jamieson S, Fuller PJ. Molecular pathogenesis of granulosa cell tumors of the ovary. Endocr Rev. 2012; 33:109–44. [PubMed: 22240241]
6. Young RH, Dickersin GR, Scully RE. Juvenile granulosa cell tumor of the ovary. A clinicopathological analysis of 125 cases. Am J Surg Pathol. 1984; 8:575–96. [PubMed: 6465418]
7. Shah SP, Kobel M, Senz J, Morin RD, Clarke BA, Wiegand KC, et al. Mutation of FOXL2 in granulosa-cell tumors of the ovary. N Engl J Med. 2009; 360:2719–29. [PubMed: 19516027]
8. Jamieson S, Butzow R, Andersson N, Alexiadis M, Unkila-Kallio L, Heikinheimo M, et al. The FOXL2 C134W mutation is characteristic of adult granulosa cell tumors of the ovary. Mod Pathol. 2010; 23:1477–85. [PubMed: 20693978]
9. Kalfa N, Ecochard A, Patte C, Duvillard P, Audran F, Pienkowski C, et al. Activating mutations of the stimulatory g protein in juvenile ovarian granulosa cell tumors: a new prognostic factor? J Clin Endocrinol Metab. 2006; 91:1842–7. [PubMed: 16507630]
10. Auguste A, Bessiere L, Todeschini AL, Caburet S, Sarnacki S, Prat J, et al. Molecular analyses of juvenile granulosa cell tumors bearing AKT1 mutations provide insights into tumor biology and therapeutic leads. Hum Mol Genet. 2015; 24:6687–98. [PubMed: 26362254]
11. Bessiere L, Todeschini AL, Auguste A, Sarnacki S, Flatters D, Legois B, et al. A Hot-spot of In-frame Duplications Activates the Oncoprotein AKT1 in Juvenile Granulosa Cell Tumors. EBioMedicine. 2015; 2:421–31. [PubMed: 26137586]
12. Liu Z, Ren YA, Pangas SA, Adams J, Zhou W, Castrillon DH, et al. FOXO1/3 and PTEN Depletion in Granulosa Cells Promotes Ovarian Granulosa Cell Tumor Development. Mol Endocrinol. 2015; 29:1006–24. [PubMed: 26061565]
13. Liu K, Rajareddy S, Liu L, Jagarlamudi K, Boman K, Selstam G, et al. Control of mammalian oocyte growth and early follicular development by the oocyte PI3 kinase pathway: new roles for an old timer. Dev Biol. 2006; 299:1–11. [PubMed: 16970938]
14. Knight PG, Glister C. TGF-beta superfamily members and ovarian follicle development. Reproduction. 2006; 132:191–206. [PubMed: 16885529]
15. Elvin JA, Yan C, Matzuk MM. Oocyte-expressed TGF-beta superfamily members in female fertility. Mol Cell Endocrinol. 2000; 159:1–5. [PubMed: 10687846]

16. Pangas SA. Bone morphogenetic protein signaling transcription factor (SMAD) function in granulosa cells. Mol Cell Endocrinol. 2012; 356:40–7. [PubMed: 21763749]
17. Schwartz NB, Channing CP. Evidence for ovarian “inhibin”: suppression of the secondary rise in serum follicle stimulating hormone levels in proestrous rats by injection of porcine follicular fluid. Proc Natl Acad Sci U S A. 1977; 74:5721–4. [PubMed: 271996]
18. Vale W, Rivier J, Vaughan J, McClintock R, Corrigan A, Woo W, et al. Purification and characterization of an FSH releasing protein from porcine ovarian follicular fluid. Nature. 1986; 321:776–9. [PubMed: 3012369]
19. Ying SY. Inhibins, activins, and follistatins: gonadal proteins modulating the secretion of follicle-stimulating hormone. Endocr Rev. 1988; 9:267–93. [PubMed: 3136011]
20. Ling N, Ying SY, Ueno N, Shimasaki S, Esch F, Hotta M, et al. Pituitary FSH is released by a heterodimer of the beta-subunits from the two forms of inhibin. Nature. 1986; 321:779–82. [PubMed: 3086749]
21. Matzuk MM, Finegold MJ, Su JG, Hsueh AJ, Bradley A. Alpha-inhibin is a tumour-suppressor gene with gonadal specificity in mice. Nature. 1992; 360:313–9. [PubMed: 1448148]
22. Cipriano SC, Chen L, Kumar TR, Matzuk MM. Follistatin is a modulator of gonadal tumor progression and the activin-induced wasting syndrome in inhibin-deficient mice. Endocrinology. 2000; 141:2319–27. [PubMed: 10875231]
23. Pierson TM, Wang Y, DeMayo FJ, Matzuk MM, Tsai SY, Omalley BW. Regulable expression of inhibin A in wild-type and inhibin alpha null mice. Mol Endocrinol. 2000; 14:1075–85. [PubMed: 10894156]
24. Pangas SA, Li X, Umans L, Zwijsen A, Huylebroeck D, Gutierrez C, et al. Conditional deletion of Smad1 and Smad5 in somatic cells of male and female gonads leads to metastatic tumor development in mice. Mol Cell Biol. 2008; 28:248–57. [PubMed: 17967875]
25. Middlebrook BS, Eldin K, Li X, Shivasankaran S, Pangas SA. Smad1-Smad5 ovarian conditional knockout mice develop a disease profile similar to the juvenile form of human granulosa cell tumors. Endocrinology. 2009; 150:5208–17. [PubMed: 19819941]
26. Li Q, Graff JM, O’Connor AE, Loveland KL, Matzuk MM. SMAD3 regulates gonadal tumorigenesis. Mol Endocrinol. 2007; 21:2472–86. [PubMed: 17595316]
27. Kim SY, Ebbert K, Cordeiro MH, Romero M, Zhu J, Serna VA, et al. Cell autonomous phosphoinositide 3-kinase activation in oocytes disrupts normal ovarian function through promoting survival and overgrowth of ovarian follicles. Endocrinology. 2015; 156:1464–76. [PubMed: 25594701]
28. Srinivasan L, Sasaki Y, Calado DP, Zhang B, Paik JH, DePinho RA, et al. PI3 kinase signals BCR-dependent mature B cell survival. Cell. 2009; 139:573–86. [PubMed: 19879843]
29. Lan ZJ, Xu X, Cooney AJ. Differential oocyte-specific expression of Cre recombinase activity in GDF-9-iCre, Zp3cre, and Msx2Cre transgenic mice. Biol Reprod. 2004; 71:1469–74. [PubMed: 15215191]
30. Kurita T, Cunha GR, Robboy SJ, Mills AA, Medina RT. Differential expression of p63 isoforms in female reproductive organs. Mech Dev. 2005; 122:1043–55. [PubMed: 15922574]
31. Pangas SA, Woodruff TK. Production and purification of recombinant human inhibin and activin. J Endocrinol. 2002; 172:199–210. [PubMed: 11786387]
32. Reed N, Millan D, Verheijen R, Castiglione M, Group EGW. Non-epithelial ovarian cancer: ESMO Clinical Practice Guidelines for diagnosis, treatment and follow-up. Ann Oncol. 2010; 21(Suppl 5):v31–6. [PubMed: 20555098]
33. Lappohn RE, Burger HG, Bouma J, Bangah M, Krans M, de Bruijn HW. Inhibin as a marker for granulosa-cell tumors. N Engl J Med. 1989; 321:790–3. [PubMed: 2770810]
34. Anttonen M, Pihlajoki M, Andersson N, Georges A, L’Hote D, Vattulainen S, et al. FOXL2, GATA4, and SMAD3 co-operatively modulate gene expression, cell viability and apoptosis in ovarian granulosa cell tumor cells. PLoS One. 2014; 9:e85545. [PubMed: 24416423]
35. Anttonen M, Unkila-Kallio L, Leminen A, Butzow R, Heikinheimo M. High GATA-4 expression associates with aggressive behavior, whereas low anti-Mullerian hormone expression associates with growth potential of ovarian granulosa cell tumors. J Clin Endocrinol Metab. 2005; 90:6529–35. [PubMed: 16159935]

36. Chang HL, Pahlavan N, Halpern EF, MacLaughlin DT. Serum Mullerian Inhibiting Substance/anti-Mullerian hormone levels in patients with adult granulosa cell tumors directly correlate with aggregate tumor mass as determined by pathology or radiology. Gynecol Oncol. 2009; 114:57–60. [PubMed: 19359032]
37. Capen CC. Mechanisms of hormone-mediated carcinogenesis of the ovary. Toxicol Pathol. 2004; 32(Suppl 2):1–5.
38. Parlow AF. Effect of Ovariectomy on Pituitary and Serum Gonadotrophins in the Mouse. Endocrinology. 1964; 74:102–7. [PubMed: 14114652]
39. Reisinger K, Baal N, McKinnon T, Munstedt K, Zygmunt M. The gonadotropins: tissue-specific angiogenic factors? Mol Cell Endocrinol. 2007; 269:65–80. [PubMed: 17349737]
40. Laronda MM, Unno K, Ishi K, Serna VA, Butler LM, Mills AA, et al. Diethylstilbestrol induces vaginal adenosis by disrupting SMAD/RUNX1-mediated cell fate decision in the Mullerian duct epithelium. Dev Biol. 2013; 381:5–16. [PubMed: 23830984]
41. Pitman JL, McNeilly AS, McNeilly JR, Hays LE, Bagby GC Jr, Sawyer HR, et al. The fate of granulosa cells following premature oocyte loss and the development of ovarian cancers. Int J Dev Biol. 2012; 56:949–58. [PubMed: 23417416]
42. Li R, Phillips DM, Mather JP. Activin promotes ovarian follicle development in vitro. Endocrinology. 1995; 136:849–56. [PubMed: 7867593]
43. Xiao S, Robertson DM, Findlay JK. Effects of activin and follicle-stimulating hormone (FSH)-suppressing protein/follistatin on FSH receptors and differentiation of cultured rat granulosa cells. Endocrinology. 1992; 131:1009–16. [PubMed: 1505447]
44. Rabinovici J, Spencer SJ, Jaffe RB. Recombinant human activin-A promotes proliferation of human luteinized preovulatory granulosa cells in vitro. J Clin Endocrinol Metab. 1990; 71:1396–8. [PubMed: 2229297]
45. Macaulay AD, Gilbert I, Caballero J, Barreto R, Fournier E, Tossou P, et al. The gametic synapse: RNA transfer to the bovine oocyte. Biol Reprod. 2014; 91:90. [PubMed: 25143353]
46. O'Hayre M, Vazquez-Prado J, Kufareva I, Stawiski EW, Handel TM, Seshagiri S, et al. The emerging mutational landscape of G proteins and G-protein-coupled receptors in cancer. Nat Rev Cancer. 2013; 13:412–24. [PubMed: 23640210]
47. Fan X, Gabbi C, Kim HJ, Cheng G, Andersson LC, Warner M, et al. Gonadotropin-positive pituitary tumors accompanied by ovarian tumors in aging female ERbeta−/− mice. Proc Natl Acad Sci U S A. 2010; 107:6453–8. [PubMed: 20308571]
48. Boerboom D, White LD, Dalle S, Courty J, Richards JS. Dominant-stable beta-catenin expression causes cell fate alterations and Wnt signaling antagonist expression in a murine granulosa cell tumor model. Cancer Res. 2006; 66:1964–73. [PubMed: 16488995]
49. Loumaye A, de Barsy M, Nachit M, Lause P, Frateur L, van Maanen A, et al. Role of Activin A and myostatin in human cancer cachexia. J Clin Endocrinol Metab. 2015; 100:2030–8. [PubMed: 25751105]
50. Petruzzelli M, Wagner EF. Mechanisms of metabolic dysfunction in cancer-associated cachexia. Genes Dev. 2016; 30:489–501. [PubMed: 26944676]

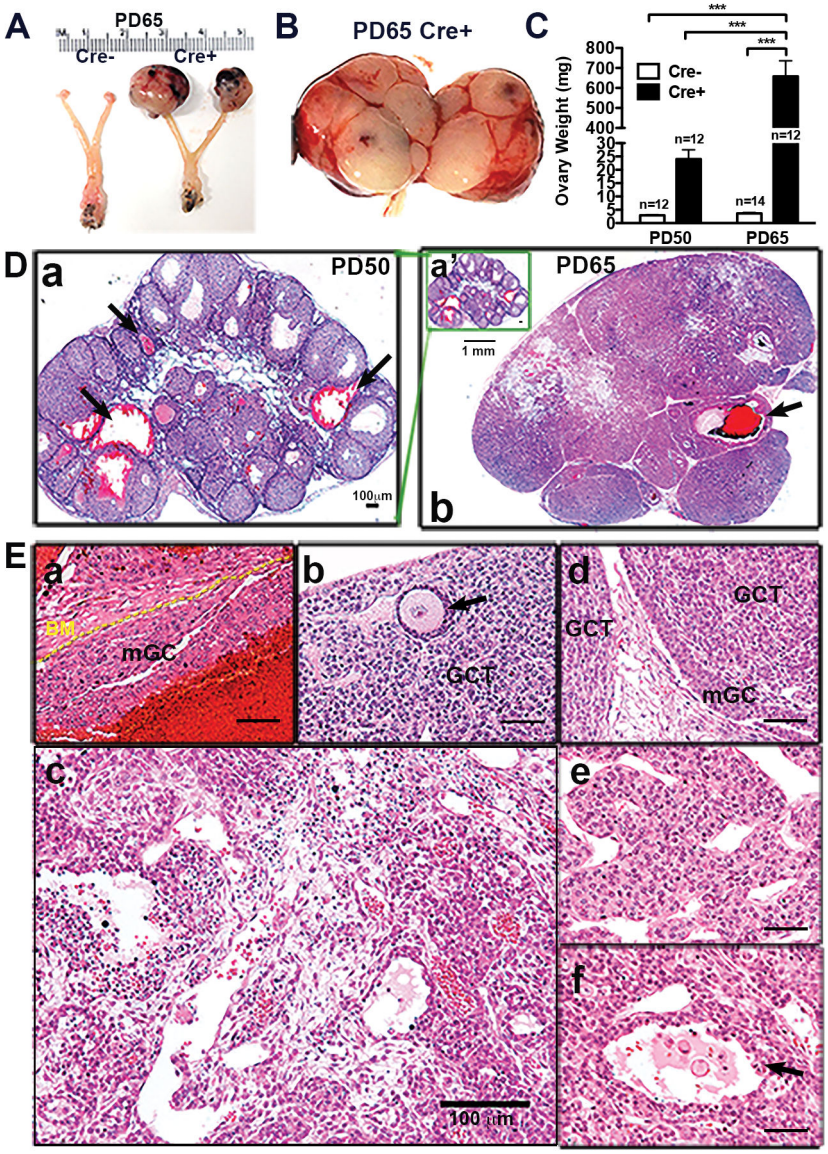

Figure 1. GCTs in Cre+ mice

(A) Female reproductive tracts from PD65 Cre− and Cre+ mice. (B) Ovarian tumors in PD65 Cre+ mice. (C) Ovarian weight of Cre− and Cre+ mice at PD50 and PD65. The difference was statistically analyzed by One-way ANOVA. (D) H&E staining of Cre+ ovaries at PD50 (a and a′) and PD65 (b). Images a′ and b are under same magnification. Multiple hemorrhagic cysts (arrows) but not tumors were present at PD50 (a and a′). At PD65, the entire ovary was filled with tumor cells (b). (E) H&E staining of PD65 Cre+ ovary. The presence of non-tumor tissues was observed, including hemorrhagic cyst within mGC and basement membrane (BM) (a), and secondary follicles (b). Tumor cells invaded stroma/connective tissues (c). Some tumor cells were contained within the mGC lining (d). GCTs typically demonstrated cord-like (e) or follicle-like (f) morphologies.

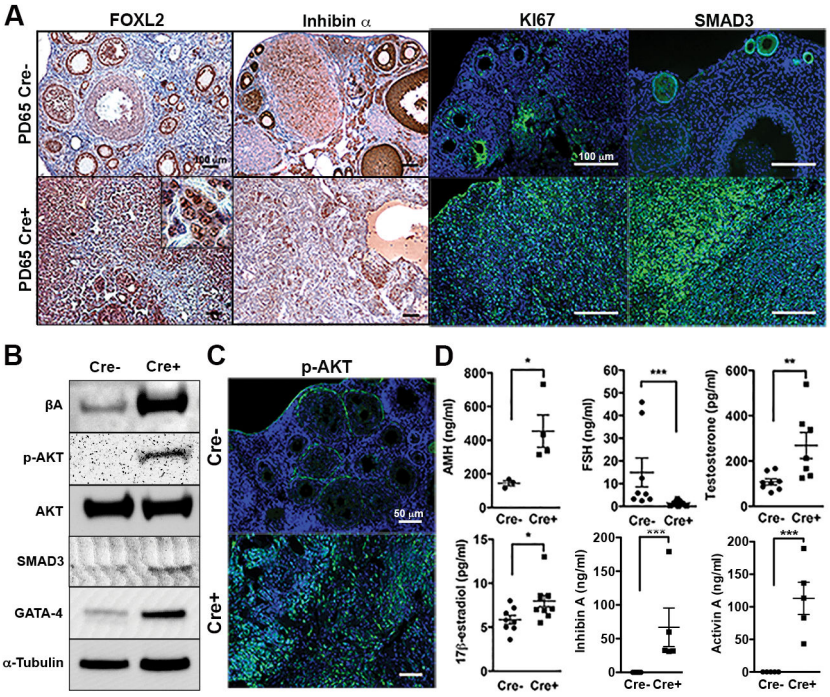

Figure 2. Molecular and endocrine characteristics of GCTs

(A) GC/GCT markers in PD65 Cre− and Cre+ ovaries. The expression of FOLX2 and inhibin α confirmed the GC origin of the cord-like cells. Note the nuclear expression of FOXL2 in the tumor cells (insert). The GCT tissues uniformly expressed KI67 and SMAD3, which were restricted to the GCs of growing follicles in Cre− ovaries. (B) Immunoblotting analysis of PD65 Cre− and Cre+ ovaries. (C) IF assay for p-AKT in PD81 Cre− and Cre+ ovaries. p-AKT was up-regulated in GCTs. (D) Serum hormone levels in PD65 Cre− and Cre+ mice. All ovarian hormones tested; AMH, testosterone, 17β-estradiol, InhA and ActA were significantly elevated, whereas FSH was significantly reduced in Cre+ mice. Difference between Cre− and Cre+ groups was analyzed by two-tailed t-test.

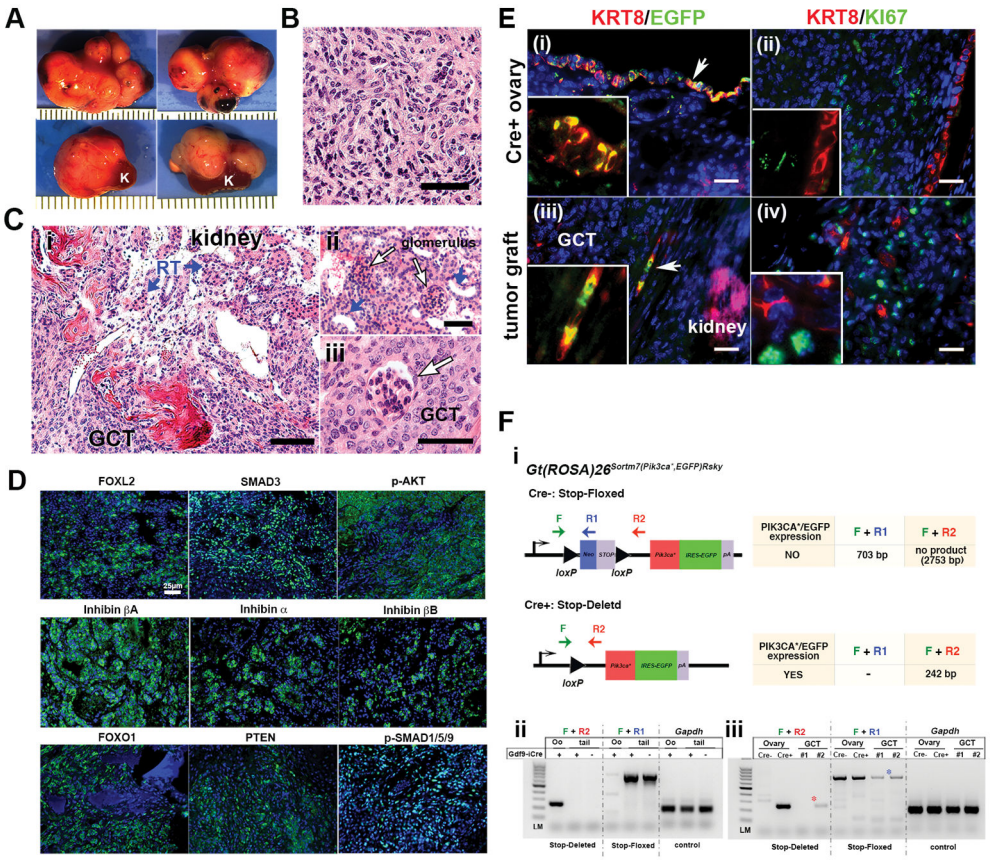

Figure 3. Characteristics of GCT transplants

(A) Appearance of GCT grafts at 35 days post-transplantation. K, kidney. (B) H&E staining of GCT transplants. Transplants maintained the histological characteristics of the original GCTs. (C) Invasion of GCT cells into host kidney. Hemorrhagic lesions at the boundary between transplants and kidney (i). Renal tubules (RTs, blue arrows) and glomeruli (white arrows) were embedded in tumor cells (ii and iii). (D) IF assay for GC markers in tumor transplants. (E) Detection of transgene expression by EGFP in PD65 Cre+ ovaries and GCT transplants. EGFP-positive somatic cells were KRT8-positive (i and iii), and KI67-negative (ii and iv). Double-positive cells for KRT8 and EGFP were indicated by arrows (i and iii). (F) Schematics of the PCR strategy for genotyping (i). Common forward primer (F) was combined with two reverse primers (R1 or R2) to detect inactive (F+R1) and active (F+R2) transgenic alleles. Specificity and sensitivity of the assay were established by positive and negative control tissues (ii). Representative results of genotyping for two different GCT transplants (#1 and #2) (iii). EGFP-positive cells were not observed in GCT#1, whereas a small number of EGFP-positive/KRT8-positive cells were detected in GCT#2. A faint band for the active transgenic allele was detected only in GCT#2.

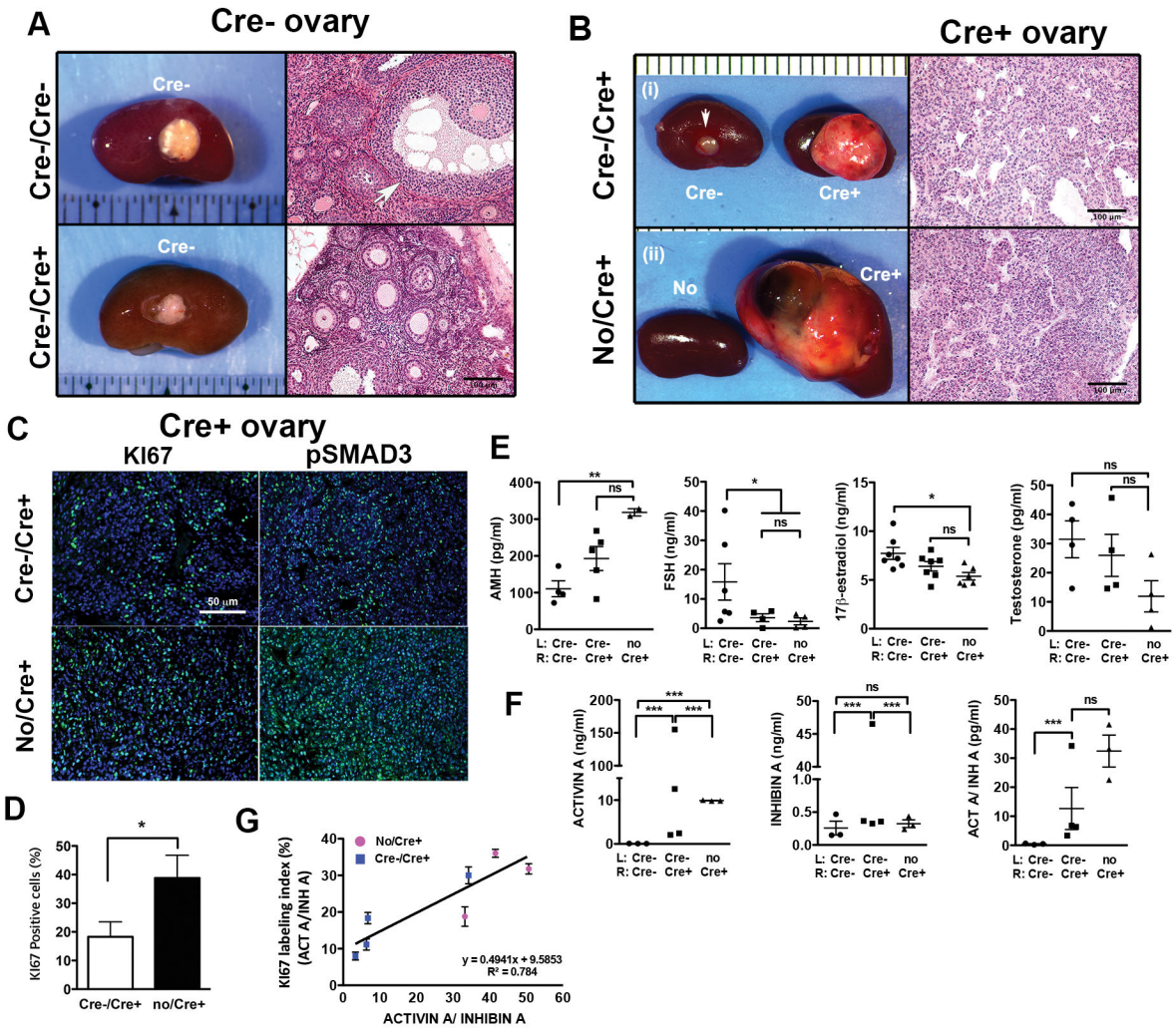

Figure 4. Co-grafting of Cre− and Cre+ immature ovaries

(A) Comparison of Cre− ovaries from Cre−/Cre− and Cre−/Cre+ groups. Cre− ovaries from Cre−/Cre+ group were less stimulated lacking large antral follicles (while arrow). (B) Comparison of Cre+ ovaries from Cre−/Cre+ and no/Cre+ groups. The GCTs were smaller and less invasive in Cre−/Cre+ than no/Cre+ groups. (C) IF assay for KI67 and p-SMAD3 in the GCTs of Cre−/Cre+ and no/Cre+ groups. (D) KI67 labeling index (percent of KI67-positive cells) in GCTs of Cre−/Cre+ and no/Cre+ groups (n=4 each). Student's t-test was performed, accounted for clustering of slide within mouse (SAS OnlineDoc® 9.4, SAS Institute Inc., Cary, NC), *P=0.048* (−/+ 17.86 mean, SE 3.40, no/+ 43.03 mean, SE 7.00). (E and F) Comparison of serum hormone levels between groups. Statistical analyses were performed with One-way ANOVA in conjunction with Tukey's Multiple Comparison Test. (G) Linear regression analysis for KI67 labeling index in GCT and serum ActA activity (ActA/InhA). Cre−/Cre+ (blue square) and no/Cre+ (pink circle) groups were plotted together. Regression line equation: y=0.4941× + 9.5853, R^2=0.784. Inclusion of inhibin B in the metrics did not affect the conclusion (supplementary Fig. S5).

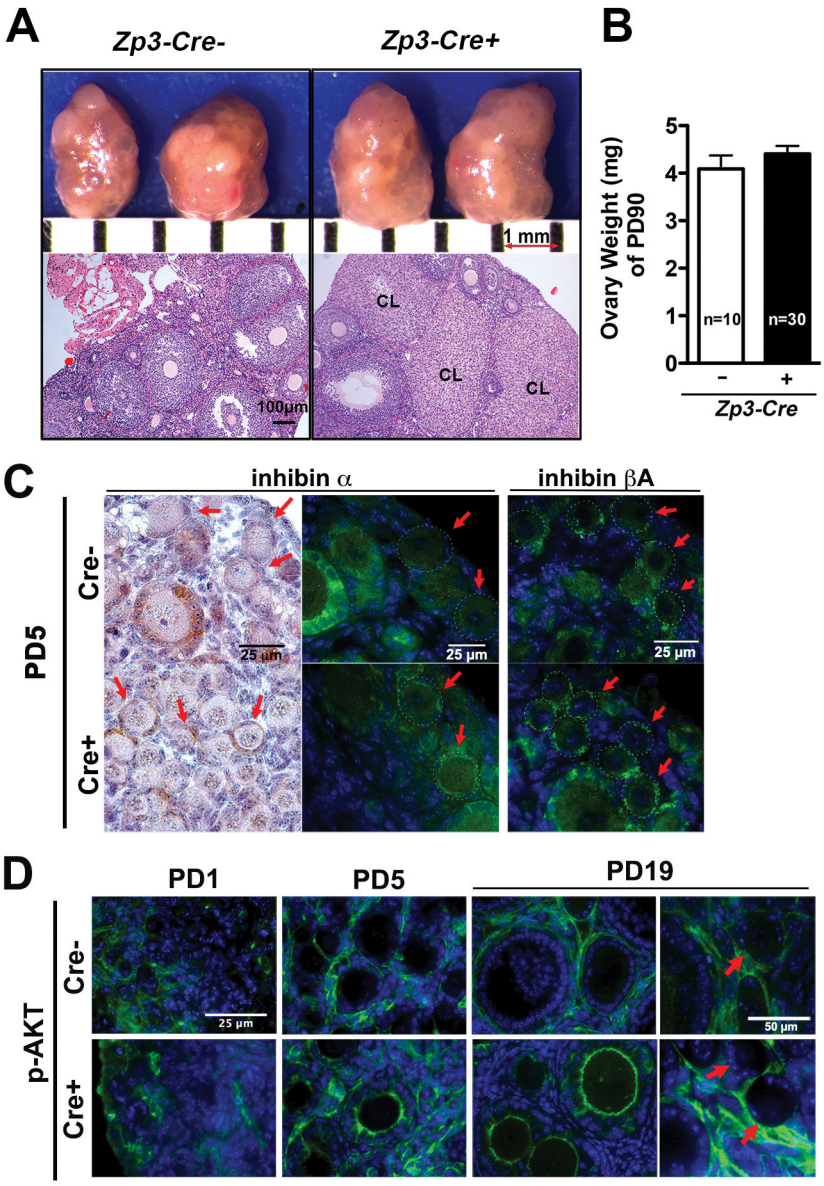

Figure 5. Effect of Cre+ oocytes on GCs during folliculogenesis

(A) Activation of *Pik3ca*-ires-EGFP* in secondary follicles by *Zp3-Cre* had no detectable effect on ovaries at PD90. CL; Corpus luteum. (B) The weight of *Zp3-Cre*− and *Zp3-Cre*+ ovaries were indistinguishable, P=0.2049 by Student's t-test. (C) Inhibin α and βA were elevated in the pregranulosa cells of PD5 Cre+ (*GDF9-iCre*+) ovaries. Primordial follicles (red arrows) are outlined with dotted lines. (D) p-AKT was elevated in Cre+ oocytes and associated GCs of activated follicles. p-AKT levels in primordial follicles were comparable in PD19 Cre− and Cre+ ovaries (red arrows).

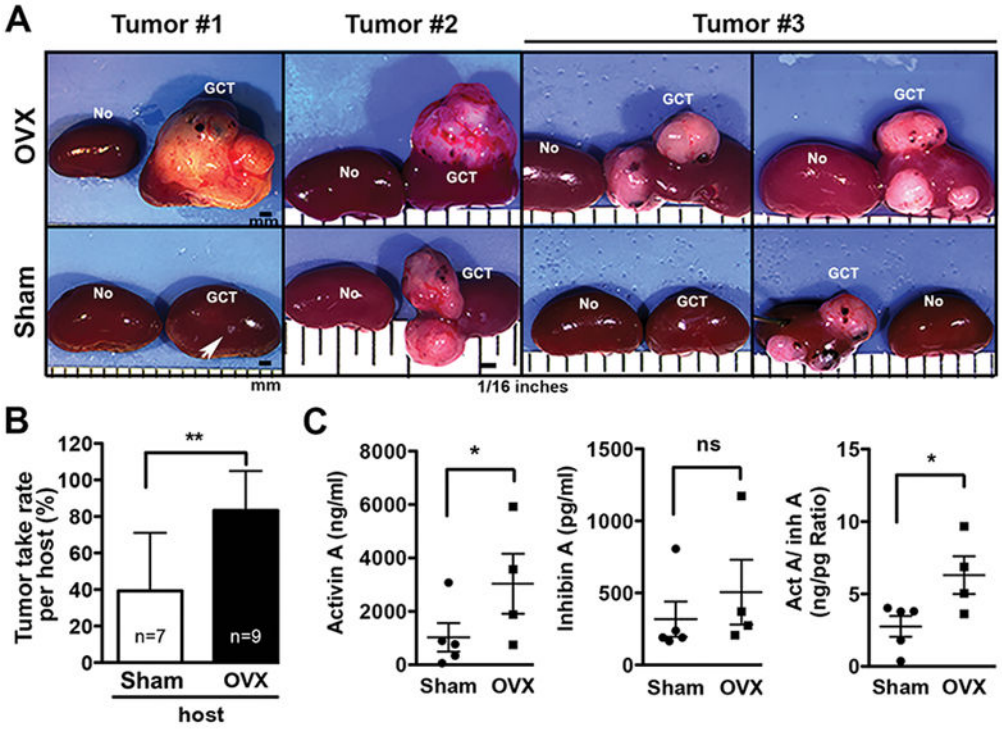

Figure 6. Effect of normal HPG axis activity on GCT growth

(A) Appearance of GCTs grown in OVX and Sham mice at 35-day post-transplantation. Tumors were marked with the ID number of the donor mice (#1–3). Each host carried 4 tumor pieces on the left kidney. GCTs grew faster in OVX than Sham hosts. A piece from GCT#1 showed no growth (white arrow). (B) Tumor take-rate. (C) Serum hormone levels of ActA and InhA in OVX and Sham hosts. Student's t-test was performed.

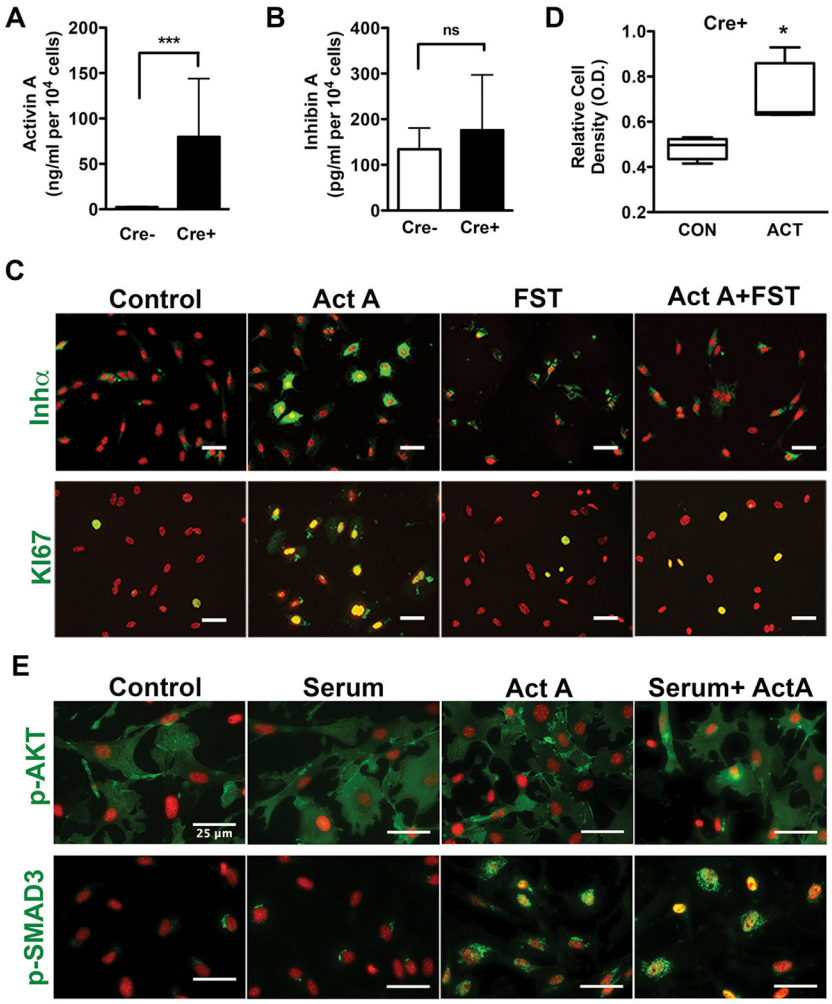

Figure 7. ActA stimulates growth of GCT cells *in vitro*

ActA (A) and InhA (B) concentrations in conditioned media (normalized to cell number). Experiments were repeated 5 times with GCs and GCT cells from 5 different mice for each genotype. (C) Immnunocytochemistry assay for inhibin α and KI67. (D) ActA effect on GCT cell growth. Cell density significantly increased with 25ng/ml ActA. Statistical analysis was performed with Student's t-test. (E) ActA effect on p-AKT and p-SMAD3 in GCT cells. While p-AKT levels were relatively constant in all treatments, the nuclear accumulation of p-SMAD3 was observed only with ActA-treatment.